Heliyon 11 (2025) e41576

Contents lists available at ScienceDirect

Heliyon

journal homepage: www.cell.com/heliyon

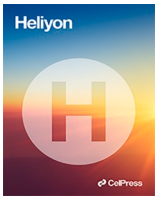

Research article

Optimizing mechanical performance: Epoxy-graphene oxide nanocomposites for enhanced strength in lattice structure

Ramezanali Gholami, Ahmad R. Khoogar *, Mohammad Hossein Allaei

Faculty of Material and Manufacturing Technologies, Malek Ashtar University of Technology, P.O. Box 1774-15875, Tehran, Iran

A R T I C L E I N F O

Keywords:
Epoxy
Graphene oxide
Nanocomposite
Mechanical properties

A B S T R A C T

The potential of epoxy-graphene oxide (GO) nanocomposites to improve the mechanical characteristics of conventional epoxy resins is causing them to gain prominence. This makes them appropriate for advanced engineering applications, including structural materials, automotive, and aerospace. This study aimed to develop an epoxy/GO composite with improved mechanical properties through synthesizing epoxy/GO samples with varying GO content (from 0.1 to 0.5 wt %), oxidation degree (from 3 to 9 g), and homogenization time (from 90 to 150 min). To do so, nine epoxy/GO composites were synthesis based on Taguchi method of experiment design (L_9 (33) orthogonal array) followed by conducting tensile strength tests. Using Taguchi method, optimal values of 0.25 wt%, 6 g, and 150 min were determined for GO content, oxidation degree, and homogenization time, respectively. Compared to tensile strength of the pure epoxy (about 38 MPa), the superior tensile strength of 73 MPa obtained for the optimal composite showcased an impressive 92 % improvement. Additionally, analysis of variance indicated the predominant role of GO's content than other parameters in improving the epoxy/GO composite's tensile strength. Finally, non-linear regression analysis was applied to develop a semi-empirical quadratic model for predicting the composite's tensile strength. The R^2 value of 99.55 % as well as a negligible AARD of 1.13 % in the optimal condition, implied the highest accuracy of developed model inside the design space.

1. Introduction

Polymeric structures have garnered considerable attention due to their remarkable versatility, ease of processing, and tailored properties. These compounds, composed of repeating units that form long chains, exhibit a wide range of characteristics that can be fine-tuned to suit specific applications [1]. As a subclass of the polymers, epoxies are defined as the most versatile and extensively available high performance materials. The excellent mechanical strength, chemical stability, and simplicity of processing of epoxy-based materials make them popular for utilizing in a variety of industries, including aerospace, marine, buildings, automotive, biomedical equipment, adhesives, and industrial equipment [2,3]. This ubiquity, however, is not without its limitations, particularly in terms of mechanical strength, durability, and overall performance. A few disadvantages, indicate that they are far from ideal; their practical uses are limited since a larger cross-link density leads to a lower strength against fractures [4]. Several studies [5,6], have come to the conclusion that a large cross-link concentration will reduce the epoxies' fracture strength because of internal stresses created during the epoxies' curing process. Low resistance to fracture formation and limited cavity growth owing to plastic

* Corresponding author.
E-mail addresses: gholami.2532@gmail.com (R. Gholami), khoogar@mut.ac.ir (A.R. Khoogar), mhallaee@gmail.com (M.H. Allaei).

https://doi.org/10.1016/j.heliyon.2024.e41576
Received 28 April 2024; Received in revised form 29 December 2024; Accepted 30 December 2024
Available online 31 December 2024

deformation are characteristics of the epoxies with a large cross-link density [7].

Amid the pursuit of overcoming the inherent drawbacks of epoxies, developing the advanced epoxy based composites by using different micro/nano fillers as an additional microphase into epoxy resin can be a promising strategy to elevate the pristine epoxies' mechanical prowess [8–10]. There are various micro/nano fillers such as metallic oxide particles [11], carbon nano tubes (CNTs) [12], silica [13,14], clays [15], and other carbonaceous materials [16–18], which widely uses as the reinforcement agent to enhance mechanical strength of the pristine epoxies. Among the carbonaceous materials, graphene is a two-dimensional carbon nanostructured compounds material that has garnered considerable fascination owing to its excessive electrical and thermal properties, exceptional strength, and extensive specific surface area [19]. However, because to its aggregation propensity, inert surface, and inadequate processability, graphene is not a good option for increasing the mechanical strength of epoxy composites. Graphene oxide (GO) is a more advantageous option that has emerged as an up-and-coming candidate. The surface of the GO is characterized by a high density of oxygen rich functional groups, including hydroxyl, carboxylic acid, carbonyl, and epoxy groups. It has the potential to strengthen the bond between GO and the resin matrix and hence increase the matrix's mechanical strength and toughness [20]. The integration of GO into polymer matrices presents a captivating avenue, promising to bridge the gap between the limitations of traditional polymers and the ever-evolving demands of modern applications [21–23]. For instance, Bortz et al. [24] also described the mechanical characteristics of GO/epoxy nanocomposites. The Young's modulus increased by 6 % at an overload of 0.5 wt%. Augmenting the loading amount demonstrated an enhancement in stiffness. The peak value of ultimate tensile strength (UTS) was observed at 0.5 wt% loading, representing a 13 % increase relative to the unmodified epoxy. The most significant enhancement was seen at modest GO concentration (<0.5 wt%) in terms of toughness and stiffness. In another study conducted by Qi et al. [25], the incorporation of 3 wt% hybrid filler, consisting of 2 wt% GO and 1 wt% liquid crystal epoxy, into the epoxy matrix led to an enhancement in tensile strength (about 27.6 %), and flexural strength (about 37.5 %). Mehrabi et al. [26] concluded that the incorporation of 0.05 phr GO into the epoxy resulted in a 34.5 % enhancement in nano-composite's elongation at break, reflecting a strong interactions between GO and epoxy at the interface, homogeneous dispersion of GO, and GO's impact on lowering the epoxy crosslinking density were all considered to be responsible for this notable increase in elongation at break. Another research conducted by Wan et al. [27] indicated that incorporation of GO nanofillers (up to 0.25 wt%) to the epoxy matrix increased the resulting composite's critical stress intensity factor (about 25.6 %), compared to pristine epoxy sample.

In recent decades, numerous investigations on enhancing the strength of epoxy/GO composites have only explored some effective characteristics, such as the GO's particle size, weight fraction, surface functionalization, and dispersion mode [28]. Studies reveal that the stoichiometric ratio between the hardener and epoxy resin is disrupted by the physical Adsorption of the resin molecules on the nanofiller's surfaces through the van der Waals interaction. On the other hand, raising the resin's temperature during the curing process results in a reduction of the resin's viscosity and facilitates the agglomeration of dispersed nanoparticles, hence diminishing the strength of the composite [4,29]. Consequently, addressing the current research gap by adjusting the homogenization time of GO nanofiller in the epoxy resin and the oxidation degree of GO which deeply affected the oxygen-containing functional group's density, would substantially change the mechanical strength of the final composite.

This study delves into the intricate realm of materials synthesis, aiming to unveil the latent potential within the epoxy-GO synergy. Within this methodical framework, the study places a spotlight on three critical variables: graphene oxide concentration, oxidation degree of graphene oxide, and mixing time. By scrutinizing the interplay among these variables, the study seeks to unravel their profound influence on the resulting mechanical properties of the epoxy-GO nanocomposite. Through the exploration of experimental complexities and analytical findings, this study develops a profound understanding of how precise manipulation of these variables can produce significant improvements in mechanical performance, highlighting the substantial influence of integrating advanced materials with systematic optimization techniques.

2. Materials and methods

2.1. Design of experiment using Taguchi method

Design of experiments (DOE) is an effective method for organizing experiments in order to examine the data as well as offer reliable and impartial findings. A comparatively straightforward and effective tool for methodical modeling, analysis, and adjustment of process variables is the Taguchi method of experiment design. It comprises variables selection, experiment execution, result analysis, identifying the optimum condition, and validation. With a series of experiments, the Taguchi technique employs a unique orthogonal array design to investigate all parameter in the design space. The experimental data are then converted into a signal-to-noise (S/N) ratio. Three stages of S/N ratio characteristics can be distinguished based on the criterion for optimizing the quality characteristic: nominal-the-better (to reduce variations near a target), larger-the-better (to maximize the system response in the design space), and smaller-the-better (to minimize the response in the design space). A higher S/N ratio indicates superior performance characteristics,

Table 1
Control parameters and their corresponding levels.

Parameters	Level 1	Level 2	Level 3
A: GO's concentration (wt.%)	0.1	0.25	0.5
B: GO's oxidation degree (g)	3	6	9
C: Homogenization time (min)	90	120	150

irrespective of the category. Consequently, the ideal parameter level corresponds to the maximum signal-to-noise ratio [30,31].

In the current research, the DOE procedure using the Taguchi method was applied by utilizing Minitab software version 14. Some effective synthesis parameters which are affected the final epoxy/GO composite's mechanical properties, such as GO's concentration, GO's oxidation degree, and homogenization time were defined as the control variables to investigate the dependency of the epoxy/GO composite's tensile strength (system response) to the mentioned control variables. The mentioned variables and their corresponding levels are reported in Table 1. Considering three factors with their corresponding three levels, the Taguchi method suggested a L_9 (33) orthogonal array, reported in Table 2, to cover the design space. To obtain the tensile testing result of the epoxy/GO composites, the composites including sample 1 to sample 9 are prepared by adjusting the control factor values in accordance with the parameters' values reported in Table 2. To obtain the highest tensile strength in the epoxy/GO composites, the tensile testing outcome was defined as the 'larger-the-better' and the S/N ratio characteristic was optimized using Equation (1).

$$S/N = -10\log\left(\frac{1}{n}\sum_{i=1}^{n}\frac{1}{y_i^2}\right) \tag{1}$$

where y_i represents the value of the tensile strength for the *i*th replication, n denotes the number of replications, and N signifies the overall quantity of the data series [30]. By analyzing the Taguchi technique's outcomes, it can be indicated that the factor level with a higher S/N ratio highlights an increased tensile strength of the resulting composite. By choosing the level with the highest S/N ratio for each component, the optimal values of the epoxy/GO synthesis condition may be determined. A validation test is then performed based on the optimal factor levels of different parameters. The validation of optimal tensile strength is performed by calculating average absolute relative deviation (AARD), presented in Equation (2).

$$AARD(\%) = \frac{100}{N}\sum_{i=1}^{N}\left(\left|\frac{Y^{Exp} - Y^{Pre}}{Y^{Exp}}\right|\right) \tag{2}$$

where, Y^{Exp}, Y^{Pre}, and N refer to experimental tensile strength, predicted tensile strength, and number of verification experiment, respectively [32].

2.2. Materials

High-purity graphite (>99.8), hydrogen peroxide (30 %), sulfuric acid (98 %), sodium nitrate (>99.5), potassium permanganate (99 % $KMnO_4$), and hydrochloric acid (37 %) were procured from Merck Company. All of the aforementioned materials were employed to synthesize the GO samples without any additional purification. Distilled water and high purity methanol (>99.9 %) were employed for washing and purification during the GO's synthesis procedure. DGEBA epoxy resin (NPEL-128, provided by Nan Ya Plastic Corp.), and EPIKURE™ F205 (manufactured by Hexion), were utilized as the matrix, and curing agent, respectively.

2.3. GO synthesis

Similar to the procedure performed by Bal [1], the GO was synthesized by the modified Hummer's method. 0.5 g of graphite powder was introduced into 65 ml of highly pure sulfuric acid, undergoing mechanical mixing for 2.5 h. Following this, the mixture underwent gradual blending with 1 g of sodium nitrate under moderate conditions. Agitation of the solution was facilitated by a mechanical mixer along with 3 g of potassium permanganate. Subsequently, the solution was left undisturbed at room temperature for 72 h, then diluted with 600 ml of deionized water and mixed for 30 min in an ice-water bath. To interrupt the oxidation reactions, hydrogen peroxide was incrementally added drop by drop to the diluted solution. This process resulted in the production of a mixture displaying a dark yellow color. The precipitated products were obtained by allowing the solution to stand still for 24 h. After undergoing several cycles of sonication and centrifugation, the sediment underwent washing three times with a 1 M hydrochloric acid solution and three times with deionized water to achieve the exfoliation of the graphite oxide sheets. The acquired sample was designated as GO3. To achieve different oxidation degrees, the same process was repeated with 6 and 9 g of potassium permanganate

Table 2
The epoxy/GO composites' synthesis parameters designed based on Taguchi method.

Sample ID	Coded value		
	GO's concentration (wt.%)	GO's oxidation degree (g)	Homogenization time (min)
1	1	1	1
2	1	2	2
3	1	3	3
4	2	1	2
5	2	2	3
6	2	3	1
7	3	1	3
8	3	2	1
9	3	3	2

which yielded the G6, and GO9 samples, respectively. A schematic figure of the GO's synthesis procedure is exhibited in Fig. 1.

2.4. Epoxy-GO synthesis

To produce the epoxy-GO nanocomposites with a 0.1 wt% GO content, about 12.9 mg GO powder was initially added to the 10.0 g epoxy resin and homogenized by utilizing a mechanical stirrer in an ice bath for 90 min. Subsequently, about 2.91 g of hardener was added to the resin and its viscosity was adjusted using ethyl acetate, followed by stirring for 5 min. The glass surfaces, intended for the application of the produced nanocomposite coating, underwent washing and degreasing. Next, a GO-epoxy composite coating was applied using a 122-μm-thick adhesive film on the pre-cleaned glass surfaces and cured for 24 h at room temperature, followed by 3 h at 122 °C. The thickness of the resulting dry layer was measured to be approximately 50 μm. To obtain free-standing films from the obtained coatings, the glass sheets were immersed in water for 2 h, and then the nanocomposite film was separated from the glass surfaces. Similar to the performed procedure, the GO-epoxy nanocomposites with the 0.25, and 0.5 wt% GO content were prepared using 32.3 mg, and 64.9 mg GO powder, respectively. A schematic figure of the epoxy/GO composite's synthesis procedure and its tensile testing apparatus is illustrated in Fig. 2.

2.5. Characterization techniques

X-ray diffraction (XRD) analysis was performed using a Phillips-PW3040/60 model X-ray diffractometer, utilizing Cu Kα radiation ($\lambda = 1.54$ Å), to examine the crystal structure and degree of oxidation of the GO. Raman spectroscopy was performed to provide insights into structural defects and functionalization degree of the GO samples. The Raman spectrums were obtained by utilizing a Takram micro Raman Spectrophotometer (Taksan™, Iran) equipped with an Argon ion laser of excitation 520 nm. Finally, to examine the mechanical properties of the epoxy nanocomposite, tensile testing was employed according to ASTM D638 standard method. This test was conducted using a Sanatam machine on free-standing films with dimensions of 52 × 1 × 12 μm at room temperature, applying a strain rate of 6 mm/min.

3. Results and discussion

3.1. The results of characterization analysis on the epoxy/GO composites

The XRD analysis was conducted to identify the crystallinity and interlayer spacing of GO, which directly affects load transfer and mechanical strength in the composite. The XRD patterns of the graphite, GO3, GO6, and GO9 samples are illustrated in Fig. 3 (a). According to this figure, the intense peak at 2θ of 26.7° corresponded to the (002) diffraction peak of graphite. This peak represented the interlayer spacing in the graphite crystal structure with d-spacing of 3.49 Å. The obtained patterns for the GO3, GO6, and GO9 samples indicated noticeable changes in the crystal structure and degree of oxidation as the amount of potassium permanganate was increased during the synthesis process. The appearance of a weaker XRD peak of the GO3 sample at 2θ of 26.4° suggested a slight change in the interlayer spacing compared to graphite. This shift indicated that the oxidation process began to affect the graphene layers, leading to the formation of graphene oxide with a lower degree of oxidation than the subsequent samples [33]. Moreover, the GO6 sample showed a broad peak at 2θ of 12.1°, signifying a significant disruption in the graphene structure. The broadening and shift towards lower angles could indicate a larger interlayer spacing due to increased oxidation. This suggested a higher degree of oxidation in the GO6 sample compared to GO3, resulting in more exfoliated graphene oxide layers. Finally, GO9 possessed the lowest 2θ with a value of 10.6°. This further shift to lower angles compared to GO6 indicated an even greater increase in interlayer spacing. GO9 sample appeared to have the highest degree of oxidation among the samples, with more exfoliated graphene oxide layers and a more disrupted crystal structure [34].

The Raman spectra of the samples are figured in Fig. 3 (b). As depicted, a prominent Raman peak emerged at a wavenumber of 1586 cm^{-1}, corresponding to the well-known G band, or graphite band. This characteristic feature indicates sp^2-hybridized carbon

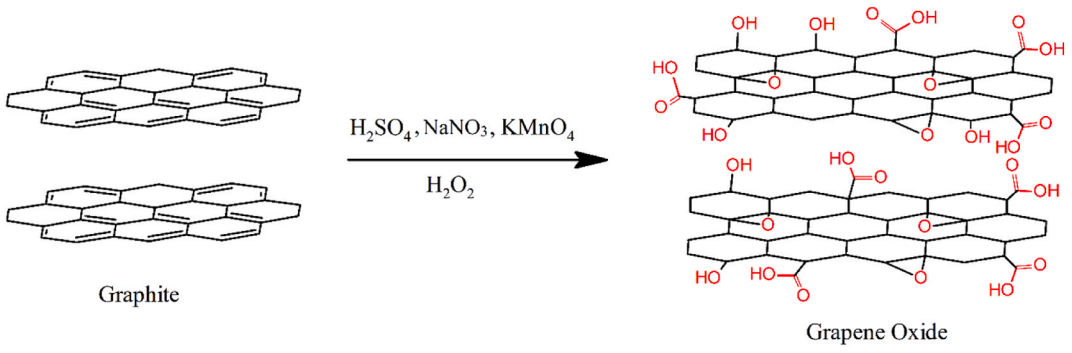

Fig. 1. GO's synthesis procedure.

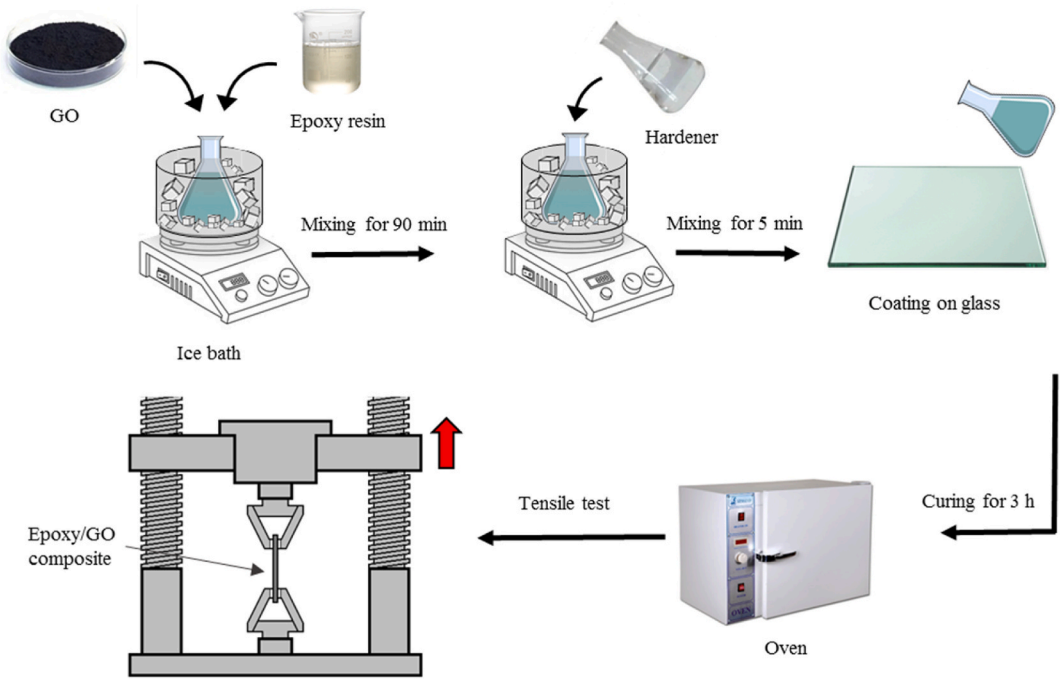

Fig. 2. The epoxy/GO composite synthesis procedure and its mechanical testing method.

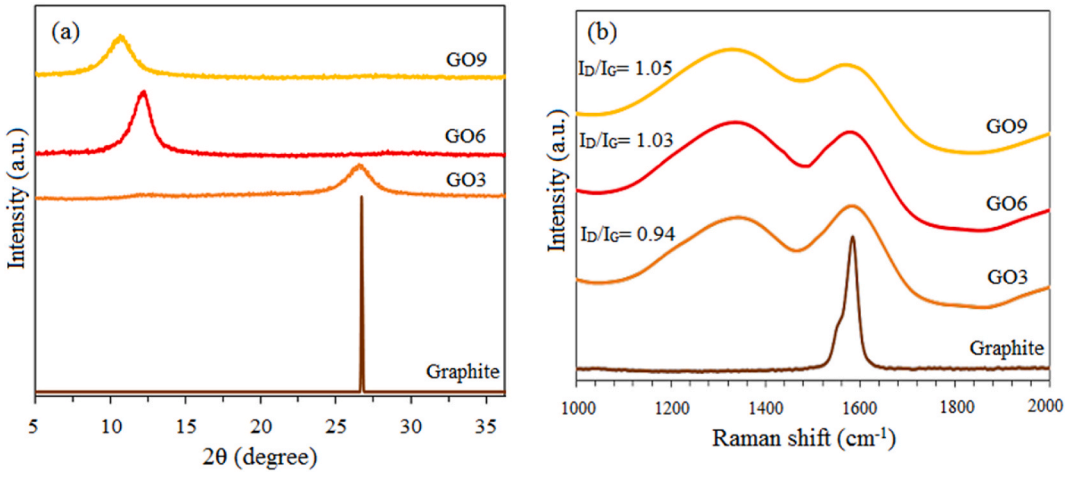

Fig. 3. Characteristic spectra of graphite, GO3, GO6, and GO9 samples obtained from a) XRD analysis, and b) Raman spectroscopy.

materials like graphene and graphite, signifying the presence of a two-dimensional hexagonal carbon lattice [35]. The G band is closely associated with in-plane vibrational modes of carbon atoms within these lattices, reflecting the stretching of carbon-carbon bonds. In the Raman spectrum of the GO3 sample, two significant Raman peaks were observed at a wavenumber of approximately 1333 and 1585 cm^{-1}. The 1333 cm^{-1} peak, known as the D band, indicates structural defects and disorder-induced during the oxidation process, possibly due to the introduction of oxygen functional groups. At 1585 cm^{-1}, the G band suggests the presence of preserved graphitic regions within the graphene oxide despite oxidation. This dual-peak pattern reveals a coexistence of disordered and oxygen-functionalized areas (D band) alongside more ordered, graphitic regions (G band) in the material, providing essential insights into its structural characteristics and oxidation degree. Moreover, the calculated intensity ratio of the D band to the G band (I_D/I_G), which is 0.94, suggested a significant presence of defects and disorder in the graphene oxide structure. A ratio approaching 1 indicates a high level of structural disruption and functionalization, emphasizing the extensive oxidation and introduction of defects [36]. Moreover, the Raman spectra of GO6 and GO9 samples revealed significant insights into their structural properties. The calculated values of I_D/I_G for GO6 and GO9 were 1.03 and 1.05, respectively, indicating a substantial level of structural disruption and defects in GO9 samples compared to other samples. This finding aligned with the higher potassium permanganate content in the synthesis

process for GO9, emphasizing the profound impact of oxidation levels on the structural characteristics of the graphene oxide samples [35].

3.2. Effect of synthesis parameters based on Taguchi method analysis

The tensile strength of the composite samples was measured based on ASTM D638 standard method, to highlight the effect of synthesis parameters. To verify the repeatability of the testing procedure and ensure reliable and accurate findings, the tensile test on composite samples was conducted three times under consistent conditions, and the average tensile strength value was recorded. A detailed information about the tensile testing result of the nine composite samples with their corresponding synthesis conditions (as coded values) are summarized in Table 3. Also, the tensile stress versus the tensile strain curves of the composite samples are shown in Fig. 4.

By implementing the Taguchi technique, the signal-to-noise (S/N) and mean values of the tensile strength of the epoxy/GO composites were calculated which are reported in Table 3. The S/N ratio of the response was calculated by utilizing 'larger-the-better' category of the performance characterization, aim to determine the composite with the highest tensile strength quantity. An elevated S/N ratio indicates enhanced performance, demonstrating less variability and diminished adverse effects [37]. Table 4 presents the average S/N ratios and mean tensile strength values associated with each level of synthesis parameters. Data from Table 4 were used to create line graphs in Fig. 5, illustrating the main effect graph of S/N ratios for the epoxy/GO composite's tensile strength. The contribution of each synthesis parameter as well as optimal condition towards obtaining the highest tensile strength are provided in the following sections.

3.2.1. Effect of GO's concentration

As shown in Fig. 5, the S/N ratio for the epoxy/GO sample's tensile strength firstly increased by improving the GO concentration up to 0.25 wt% followed by a gradually reduction in higher amount of GO concentration up to 0.5 wt%. Compare to the tensile strength of the pure epoxy obtained around 38 MPa (young modulus of 622 MPa), it can be concluded that introduction of GO, even at a low concentration of 0.1 wt%, enhanced the mechanical properties of the nanocomposite. The unique two-dimensional structure of graphene oxide, with its high aspect ratio and excellent mechanical properties, reinforced the epoxy matrix. The functional groups on the surface of GO sheets facilitated strong interactions with the epoxy matrix, resulting in improved load transfer between the polymer matrix and the nanofillers [38]. Although a higher crosslink density in epoxy materials is advantageous for enhancing mechanical characteristics, nonetheless, elevated crosslink density adversely impacts fracture toughness and a threshold for crosslink density is necessary to get optimum characteristics [39]. During the curing procedure of epoxy polymers, GO sheets prefer to cluster to minimize configurational entropy while phase change occurs. Furthermore, the viscosity decreases initially with a rise in temperature during the curing process, facilitating the mobility of the GO sheets and promoting their agglomeration. The wrinkled morphology and elevated specific surface area of GO facilitate robust interfacial interactions with epoxy chains. It may also influence the total curing reaction by altering the highest exothermic heat release [28,39]. Despite a positive effect of introducing GO particles towards improving the composite's tensile strength, the outcomes exhibited in Fig. 4 highlights a significant change in strain at break for composites. For example, the observed decrease in strain at break for the sample 1 (4.7 %) compared to pure epoxy (6.1 %) suggested a reduction in the material's ductility. This phenomenon could be attributed to the reinforcing effects of GO in the nanocomposite. While GO contributed to increased stiffness, its inherent rigidity may limit the material's ability to deform extensively before failure [40,41]. The incorporation of GO, even at a low concentration of 0.1 wt%, may lead to a more brittle behavior in the nanocomposite, as evidenced by the reduced strain at break.

3.2.2. Effect of GO's oxidation degree

As shown in Fig. 5, the S/N ratios for tensile strength of the epoxy/GO composites versus the GO's oxidation degree indicates that the composite sample containing GO6 nanoparticles exhibited the maximum tensile strength. As the oxidation degree of the GO increased (up to 9), the tensile strength of the resultant composite diminished progressively. This effect may be ascribed to the increased density of oxygen-containing functional groups on the surface of graphene oxide, which enhances the surface potential energy and therefore renders the surface heterogeneous [42]. The heterogeneous surface of the GO may adsorb epoxy molecules via a

Table 3
Tensile strengths of different samples with different synthesis conditions.

Run	Coded value			Tensile strength (MPa)				
	GO's conc.	GO's oxidation	Homogen. time	Trial 1	Trial 2	Trial 3	Mean	S/N
1	1	1	1	40.6	39.6	39.9	40.0	32.05
2	1	2	2	44.3	44.1	43.7	44.0	32.88
3	1	3	3	40.3	41.3	41.5	41.0	32.26
4	2	1	2	50.1	51.5	51.5	51.0	34.15
5	2	2	3	71.6	74.1	73.4	73.0	37.27
6	2	3	1	52.2	53.3	53.7	53.0	34.49
7	3	1	3	46.9	48.8	48.4	48.0	33.63
8	3	2	1	54.6	54	53.4	54.0	34.65
9	3	3	2	48.9	48.6	49.5	49.0	33.80

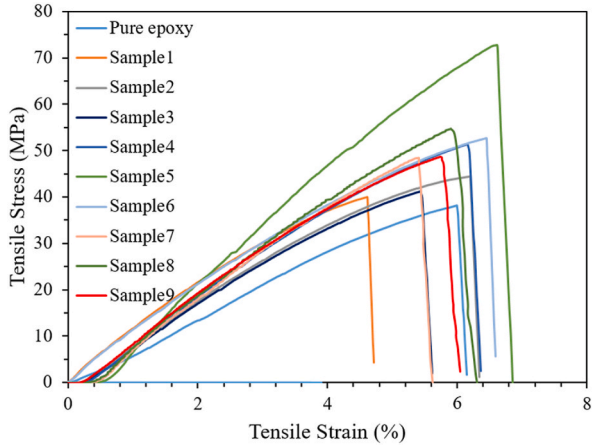

Fig. 4. Stress-strain curves of pure epoxy and epoxy/GO composites.

Table 4
Response table for S/N ratios for the epoxy/GO composite's tensile strength.

Level	GO conc. (wt.%)	GO oxidation (g)	Mixing time (min)
1	32.39	33.28	33.73
2	**35.31**	**34.93**	33.61
3	34.03	33.52	**34.39**
Delta (max-min)	2.91	1.65	0.77
Rank	1	2	3

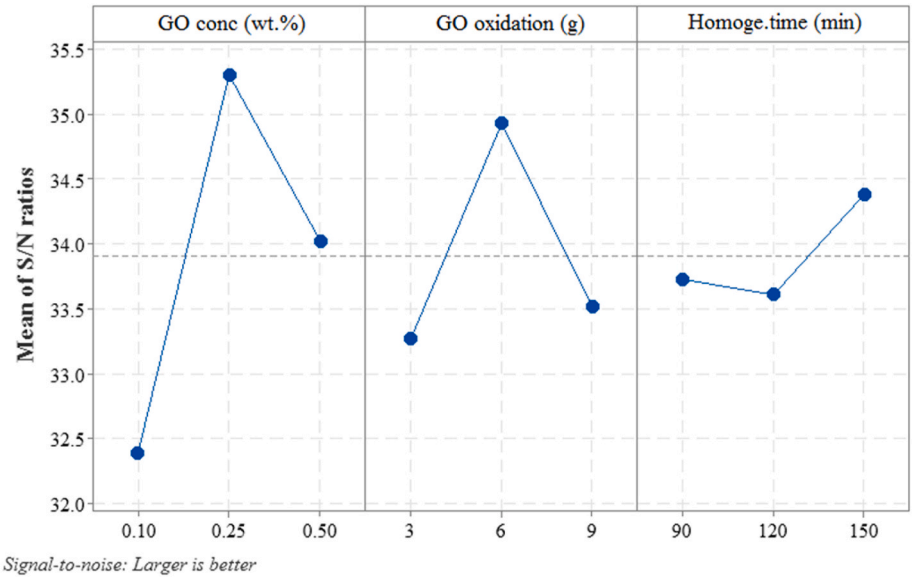

Fig. 5. Main effect graphs of S/N rations for the epoxy/GO composite's tensile strength versus control parameters.

physisorption process due to enhanced van der Waals interactions, resulting in disruption of the stoichiometric ratio between the epoxy resin and the hardener, and incomplete cross-linking [4,29].

3.2.3. Effect of homogenization time

Considering the S/N ratios corresponding to homogenization time, summarized in Table 4, it could be resulted that increasing in homogenization time up to 120 min, firstly reduced the tensile strength of the composite followed by increasing in larger homogenization time. The highest S/N ratio of this parameter imply that higher homogenization time (up to 150) can yielded the highest

tensile strength in the resulting composite sample. This behavior may be attributed to the effective dispersion of GO nanoparticles inside the epoxy matrix due to extended homogenization time, which prevents the agglomeration of the nanoparticles [43]. While extending the homogenization time improves the dispersion of GO and enhances the mechanical strength of the composites, some literature suggests that excessive sonication time is unwarranted as it can cause localized destruction to GO platelets, including bending and breakage [29,43].

3.2.4. Optimal condition for epoxy/GO synthesis

Considering the outcome mentioned earlier, an intricate relationship can be highlighted between GO concentration, oxidation degree, homogenizing time, and the resulting mechanical performance in epoxy/GO nanocomposites. The variations in tensile strength among the samples highlighted the importance of tailoring these parameters for achieving desired mechanical characteristics. The optimal synthesis condition based on the Taguchi method was obtained through selecting the highest S/N ratio for each parameter, as reported in Table 4 in bold format. In this table, delta refer to the differences between maximum and minimum quantity of the S/N ratio and the order of significance for the synthesis parameters towards improving the tensile strength are acquired based on magnification of delta values [44]. The optimal synthesis condition was obtained for level 2, level 2, and level 3 of GO's concentration, GO's oxidation degree, and homogenization time, respectively. In the optimum condition (corresponding to sample 5's synthesis condition), the experimental tensile strength was recorded around 73.0 MPa while the calculated amount of this feature based on the Taguchi design was obtained around 69.37 MPa. The Taguchi design accuracy was checked by calculating the average absolute relative deviation (AARD) which yielded a minor AARD around 4.98 %. The minor AARD value highlights a good accuracy of the Taguchi method for predicting the composite's tensile strength in the optimal condition.

3.3. Analysis of variance

The conventional statistical ANOVA helps to analyze the Taguchi method precision for predicting S/N ratios for tensile strength as well as determining which synthesis parameters substantially influence the response. ANOVA is performed to discover significant parameters at a confidence level of 0.95, which corresponds to a significance level of 0.05. The ANOVA outcomes are reported in Table 5. In this table, the contribution of each parameter is summarized in the last column of table which was calculated by dividing the sum of squares of each variable to the total sum of squares. The P-values less than 0.05, and the F-values more than 1 may also be used to ascertain which parameter significantly influences the model's response [45]. Considering the P-value obtained for GO's concentration (0.0071), it can be concluded that this term has the highest impact on the resulting composite's mechanical properties. This finding has good accordance whit its contribution percentage obtained about 65.28 %. Although the P-values for other parameters are more than 0.05, the F-values more than 1 for GO's oxidation degree and the homogenization time indicate their moderated significance which have good accordance with their contribution percentage obtained around 24.44 %, and 5.33 %, respectively. The correlation coefficient of the linear model was obtained about 95.04 %, but the adjusted R^2 values of 80.18 % highlights inadequate accuracy of the model in forecasting the composite's tensile strength within the design space. This outcome may be attributed to ignoring the interaction terms which may exist between parameters.

3.4. Non-linear regression model

As mentioned earlier, a possible interaction between the syntheses parameters can affected the tensile strength of the composite sample and these terms could not be considered by linear model [46]. Therefore, using 'Fit regression model' tool of Minitab software, the non-linear regression was performed in the confidence level of 0.95, to consider the interaction term as well as the quadratic terms of each parameter. The quadratic model terms' coefficient and their statistical analysis results are reported in Table 6. In this table the terms A, B, and C, refer to the parameters namely GO's concentration, GO's oxidation degree, and homogenization time, respectively. Also the resulting quadratic model is presented in equation (3). According to the finding summarized Table 6, the predominance impact of quadratic terms (A^2, B^2, and C^2) in predicting tensile strength could be observed due to their higher F-values. Considering the P-values, the significant effect of model terms could be highlighted except for the interaction term between GO's concentration and homogenization time (P-value more than 0.05). The adjusted R^2 of the model (99.35 %) has less than 20 % differences with the predicted R^2 (98.99 %), implying the highest accuracy of the resulting quadratic model towards forecasting the tensile strength inside the design space. To further validate the model's precision, the model predicted tensile strength was rechecked in the optimal condition obtained base on Taguchi method. The model predicted tensile strength of 73.04 MPa indicated a negligible AARD of 1.13 %

Table 5
ANOVA results for S/N ratios for the epoxy/GO composite's tensile strength.

Source	Degree of freedom	Sum of square	Mean square	F- value	P-value	Contribution (%)
GO's concentration	2	12.7764	6.3882	13.17	0.0071	65.28
GO's oxidation degree	2	4.7829	2.3915	4.93	0.1686	24.44
Homogenization time	2	1.0430	0.5215	1.08	0.4818	5.33
Residual Error	2	0.9699	0.4849			4.95
Total	8	19.5722				100

$R^2 = 95.04$ %. Adjusted $R^2 = 80.18$ %.

Table 6
ANOVA results for non-linear model terms.

Source	Degree of freedom	Sum of square	Mean square	F- value	P-value
Regression	8	2328.08	291.01	497.61	0.0000
A	1	287.92	287.92	492.33	0.0000
B	1	244.47	244.47	418.03	0.0001
C	1	179.77	179.77	307.40	0.0003
A^2	1	1168.98	1168.98	1998.88	0.0000
B^2	1	454.67	454.67	777.46	0.0000
C^2	1	198.53	198.53	339.47	0.0002
A*B	1	162.04	162.04	277.08	0.0005
A*C	1	1.61	1.61	2.75	0.1149
Error	18	10.53	0.58		
Total	26	2338.60			

$R^2 = 99.55$ %. Adjusted $R^2 = 99.35$ %. Predicted $R^2 = 98.99$ %.

with the experimental tensile strength quantity of 73.0 MPa in the optimum condition.

$$\text{Tensile strength (MPa)} = 87.35 + 183.81\,A + 11.562\,B + 8.819\,A*B + 0.0878\,A*C - 1.6789C - 376.07\,A^2 - 1.1465\,B^2 + 0.007576C^2 \quad (3)$$

3.5. Comparison between current study outcomes and similar works

Table 7 presents the findings of analogous investigations about the increase of mechanical characteristics in epoxy nanocomposites with various nano-fillers. The results gathered from the table demonstrate that the epoxy/GO composite created in this work exhibits much greater tensile strength than those reported in comparable investigations. This finding underscores the key importance of the synthesis conditions of GO, along with other key parameters such as homogenization duration and the loading % of GO.

4. Conclusion

The present research's findings indicate that the mechanical properties of the epoxy/GO nanocomposites can be significantly enhanced through the careful optimization of key factors, including GO content, time of homogenization, and the oxidation degree of GO. The influence of these parameters on tensile strength has been rigorously confirmed by empirical data and the Taguchi method analysis. The regression analysis demonstrated a non-linear effect of GO's concentration on tensile strength. A gradual improvement in strength was observed as the GO content increased to 0.25 wt%, followed by a decline when the concentration reached 0.5 wt%. This suggests the importance of careful regulation of GO content to prevent excessive agglomeration and maintain a balance between crosslink density and fracture toughness. Similarly, the homogenization time is critical to the uniform dispersion of GO nanoparticles in the epoxy matrix. Prolonged homogenization time (up to 150 min) improved the dispersion of nanoparticles, resulting in a significant rise in tensile strength. Likewise, the degree of oxidation demonstrated a substantial impact on the mechanical properties of the composite. Enhanced oxidation brings about functional groups that enhance interfacial bonding with epoxy chains; however, excessive oxidation leads to disrupted crosslinking, ultimately undermining the tensile strength of the composite. The findings collectively demonstrate the potential for precise adjustments of these parameters to improve the mechanical performance of epoxy-GO nanocomposites, thereby broadening their applicability in engineering fields.

CRediT authorship contribution statement

Ramezanali Gholami: Writing – review & editing, Validation, Software. **Ahmad R. Khoogar:** Writing – original draft, Supervision. **Mohammad Hossein Allaei:** Writing – review & editing, Resources.

Data availability statement

Data will be made available on request.

Additional information

No additional information is available for this paper.

Declaration of competing interest

The authors declare that they have no known competing financial interests or personal relationships that could have appeared to influence the work reported in this paper.

Table 7
Mechanical properties improvement in the epoxy/nano-particles (NP) composites.

Researcher	NP type	NP Loading (wt%)	Homogenization method	Tensile strength enhancement (%)	Ref
Mirzapour et al.	GO	0.6	Mechanical mixing	46.0	[47]
Katti et al.	Epoxy grafted GO	0.5	Mechanical mixing- sonication	8.0	[48]
Wang et al.	TiO_2-rGO	0.2	Mechanical mixing	75.5	[49]
Kavimani et al.	rGO-montmorillonite	0.2	Mechanical mixing	78.5	[50]
Hao et al.	GO-SiO_2	0.1	auxiliary thermal blending	38.6	[51]
Jiang et al.	APTES grafted SiO_2-GO	0.5	Mechanical mixing- sonication	18.8	[52]
Cao et al.	Gallic acid modified GO	2	Sonication	21.2	[53]
Gholami et al.	GO	0.25	Mechanical mixing	92	This work

References

[1] S. Bal, Experimental study of mechanical and electrical properties of carbon nanofiber/epoxy composites, Mater. Des. (1980-2015) 31 (5) (2010) 2406–2413.
[2] R. Sahay, V.J. Reddy, S. Ramakrishna, Synthesis and applications of multifunctional composite nanomaterials, Int. J. Mech. Mater. Eng. 9 (1) (2014) 25.
[3] T. Cuong-Le, et al., Nonlocal strain gradient IGA numerical solution for static bending, free vibration and buckling of sigmoid FG sandwich nanoplate, Phys. B Condens. Matter 631 (2022) 413726.
[4] N. Domun, et al., Improving the fracture toughness and the strength of epoxy using nanomaterials–a review of the current status, Nanoscale 7 (23) (2015) 10294–10329.
[5] A.C. Garg, Y.-W. Mai, Failure mechanisms in toughened epoxy resins—a review, Compos. Sci. Technol. 31 (3) (1988) 179–223.
[6] R. Pearson, A. Yee, Toughening mechanisms in elastomer-modified epoxies: Part 3 the effect of cross-link density, J. Mater. Sci. 24 (1989) 2571–2580.
[7] M. Martin-Gallego, et al., Epoxy nanocomposites filled with carbon nanoparticles, Chem. Rec. 18 (7–8) (2018) 928–939.
[8] M.S. Rabbi, T. Islam, G.M.S. Islam, Injection-molded natural fiber-reinforced polymer composites–a review, Int. J. Mech. Mater. Eng. 16 (1) (2021) 15.
[9] J. Passantino, A. Haywood, J. Goswami, V. Davis, Effects of polymer additives and dispersion state on the mechanical properties of cellulose nanocrystal films, Macromol. Mater. Eng. 302 (2017) 1600351.
[10] C.L. Thanh, et al., A geometrically nonlinear size-dependent hypothesis for porous functionally graded micro-plate, Eng. Comput. 38 (1) (2022) 449–460.
[11] W. Naous, et al., Morphology, tensile properties, and fracture toughness of epoxy/Al2O3 nanocomposites, J. Polym. Sci. B Polym. Phys. 44 (10) (2006) 1466–1473.
[12] I. Srikanth, et al., Effect of amino functionalized MWCNT on the crosslink density, fracture toughness of epoxy and mechanical properties of carbon–epoxy composites, Compos. Appl. Sci. Manuf. 43 (11) (2012) 2083–2086.
[13] C.F. Ou, M.C. Shiu, Epoxy composites reinforced by different size silica nanoparticles, J. Appl. Polym. Sci. 115 (5) (2010) 2648–2653.
[14] P. Snopiński, et al., Engineering an ultra-fine grained microstructure, twins and stacking faults in PBF-LB/M Al-Si alloy via KoBo extrusion method, J. Alloys Compd. 970 (2024) 172576.
[15] W. Liu, S.V. Hoa, M. Pugh, Fracture toughness and water uptake of high-performance epoxy/nanoclay nanocomposites, Compos. Sci. Technol. 65 (15–16) (2005) 2364–2373.
[16] J. Guest, I.A. Kinloch, R.J. Young, The role of filler aspect ratio in the reinforcement of an epoxy resin with graphene nanoplatelets, J. Mater. Sci. 58 (23) (2023) 9473–9485.
[17] O. Vryonis, et al., Understanding the cross-linking reactions in highly oxidized graphene/epoxy nanocomposite systems, J. Mater. Sci. 54 (4) (2019) 3035–3051.
[18] P. Phung-Van, et al., Nonlocal strain gradient analysis of honeycomb sandwich nanoscale plates, Thin-Walled Struct. 198 (2024) 111746.
[19] A. Vashchuk, et al., Thermal conductivity and mechanical properties of epoxy vitrimer nanocomposites reinforced with graphene oxide, Appl. Nanosci. 13 (7) (2023) 4675–4683.
[20] L. Cao, et al., Synergistically improving mechanical and interfacial properties of epoxy resin and CFRP composites by introducing graphene oxide, Adv. Polym. Technol. 2022 (1) (2022) 8309259.
[21] A. Ammar, A.M. Al-Enizi, M.A. AlMaadeed, A. Karim, Influence of graphene oxide on mechanical, morphological, barrier, and electrical properties of polymer membranes, Arab. J. Chem. 9 (2) (2016) 274–286.
[22] A.K. Pathak, et al., Improved mechanical properties of carbon fiber/graphene oxide-epoxy hybrid composites. Composites Science and Technology 135 (2016) 28–38.
[23] C. Shuai, et al., A graphene oxide-Ag co-dispersing nanosystem: Dual synergistic effects on antibacterial activities and mechanical properties of polymer scaffolds, Chem. Eng. J. 347 (2018) 322–333.
[24] D.R. Bortz, E.G. Heras, I. Martin-Gullon, Impressive fatigue life and fracture toughness improvements in graphene oxide/epoxy composites, Macromolecules 45 (1) (2012) 238–245.
[25] B. Qi, et al., Mechanical and thermal properties of epoxy composites containing graphene oxide and liquid crystalline epoxy, Fibers Polym. 15 (2) (2014) 326–333.
[26] M. Mehrabi-Kooshki, A. Jalali-Arani, Preparation of binary and hybrid epoxy nanocomposites containing graphene oxide and rubber nanoparticles: fracture toughness and mechanical properties, J. Appl. Polym. Sci. 136 (4) (2019) 46988.
[27] Y.-J. Wan, et al., Grafting of epoxy chains onto graphene oxide for epoxy composites with improved mechanical and thermal properties, Carbon 69 (2014) 467–480.
[28] R. Atif, I. Shyha, F. Inam, Mechanical, thermal, and electrical properties of graphene-epoxy nanocomposites—a review, Polymers 8 (8) (2016) 281.
[29] S. Rana, R. Alagirusamy, M. Joshi, Development of carbon nanofibre incorporated three phase carbon/epoxy composites with enhanced mechanical, electrical and thermal properties, Compos. Appl. Sci. Manuf. 42 (5) (2011) 439–445.
[30] S. Navaneethakrishnan, A. Athijayamani, Taguchi method for optimization of fabrication parameters with mechanical properties in fiber and particulate reinforced composites, Int. J. Plast. Technol. 19 (2) (2015) 227–240.
[31] B. Pratap, V.K. Patel, Synergy of hybridization of bauhinia vahlii and kenaf fiber on mechanical and sliding wear properties of epoxy composites: a Grey Taguchi Optimization Study, Heliyon 10 (3) (2024) e25868.
[32] M.R. Moradi, H. Ramezanipour Penchah, A. Ghaemi, CO capture by benzene-based hypercrosslinked polymer adsorbent: Artificial neural network and response surface methodology, Can. J. Chem. Eng. 101 (10) (2023) 5621–5642.
[33] J. Fan, et al., Cryogenic mechanical properties of graphene oxide/epoxy nanocomposites: influence of graphene oxide with different oxidation degrees, Polym. Test. 96 (2021) 107074.
[34] Y. Wei, et al., Influence of graphene oxide with different oxidation levels on the properties of epoxy composites, Compos. Sci. Technol. (2018) 161.
[35] J. Guerrero-Contreras, F. Caballero-Briones, Graphene oxide powders with different oxidation degree, prepared by synthesis variations of the Hummers method, Mater. Chem. Phys. 153 (2015) 209–220.
[36] K. Krishnamoorthy, M. Veerapandian, K. Yun, S.J. Kim, The chemical and structural analysis of graphene oxide with different degrees of oxidation, Carbon 53 (2013) 38–49.
[37] M.A. Islam, et al., Soft material drilling: a thermo-mechanical analysis of polyurethane foam for biomimetic bone scaffolds and optimization of process parameters using Taguchi method, Heliyon 10 (17) (2024) e37465.

[38] K. Zeng, et al., Investigation of mechanical and thermal characteristics of epoxy/graphene oxide nanocomposites by molecular dynamics simulation, Mater. Sci. Eng., B 287 (2023) 116087.
[39] X. Wang, J. Jin, M. Song, An investigation of the mechanism of graphene toughening epoxy, Carbon 65 (2013) 324–333.
[40] D. Galpaya, et al., Preparation of graphene oxide/epoxy nanocomposites with significantly improved mechanical properties, J. Appl. Phys. 116 (5) (2014).
[41] H. Yang, et al., Convenient preparation of tunably loaded chemically converted graphene oxide/epoxy resin nanocomposites from graphene oxide sheets through two-phase extraction, J. Mater. Chem. 19 (46) (2009) 8856–8860.
[42] P. Rostami, M.R. Moradi, M. Ashourzadeh Pordsari, A. Ghaemi, Carboxylic acid functionalized para-xylene based hypercrosslinked polymer as a novel and high performance adsorbent for heavy metal removal, Arab. J. Chem. 17 (4) (2024) 105634.
[43] G.H. Majzoobi, S.H.A. Nejad, S.A.R. Sabet, Role of graphene oxide and sonication time on mechanical properties of epoxy nanocomposites at high strain rate, Mater. Res. Express 6 (6) (2019) 65063.
[44] T.A. Miliket, M.B. Ageze, M.T. Tigabu, M.A. Zeleke, Experimental characterizations of hybrid natural fiber-reinforced composite for wind turbine blades, Heliyon 8 (3) (2022) e09092.
[45] M. Ashourzadeh Pordsari, M. Moradi, A. Ghaemi, Fabrication of a cost-effective metal oxide-based adsorbent from industrial waste slag for efficient CO2 separation under flue gas conditions, J. CO2 Util. 88 (2024) 102930.
[46] K. Sudarshan Rao, Taguchi and regression analysis of abrasive wear behavior of carbon epoxy composite, J. Mater. 1 (2) (2023) 68–73.
[47] M. Mirzapour, M. Robert, B. Benmokrane, In situ processing to achieve high-performance epoxy nanocomposites with low graphene oxide loading, C 10 (2) (2024) 52.
[48] P. Katti, K.K. Verma, S. Kumar, S. Bose, Tuning the interface in epoxy-based composites and laminates through epoxy grafted graphene oxide enhances mechanical properties, Nanoscale Adv. 3 (23) (2021) 6739–6749.
[49] Y. Wang, S. Guo, B. Dong, F. Xing, Enhanced tensile strength of monolithic epoxy with highly dispersed TiO2-graphene nanocomposites, J. Compos. Sci. 5 (7) (2021) 191.
[50] V. Kavimani, et al., Application of r-GO-MMT hybrid Nanofillers for improving Strength and flame Retardancy of epoxy/glass fibre composites, Adv. Polym. Technol. 2021 (1) (2021) 6627743.
[51] Q. Hao, et al., Preparation of GO-SiO three-dimensional point-plane nanomaterials and enhancement of epoxy resin mechanical property, Polym. Compos. 45 (2) (2024) 1266–1277.
[52] T. Jiang, T. Kuila, N.H. Kim, J.H. Lee, Effects of surface-modified silica nanoparticles attached graphene oxide using isocyanate-terminated flexible polymer chains on the mechanical properties of epoxy composites, J. Mater. Chem. A 2 (27) (2014) 10557–10567.
[53] L. Cao, et al., How a bio-based epoxy monomer enhanced the properties of diglycidyl ether of bisphenol A (DGEBA)/graphene composites, J. Mater. Chem. A 1 (16) (2013) 5081–5088.